抄録

発表者氏名	タイトル名	学会名	開催日
Osai Y, Tamura Y, Sato N, Wakamatsu K, Ito S, Ito A, Honda H, Ohkura M, Yamashita T, Jimbow K	N-propionyl-cysteaminylphenol suppresses re-challenge of mouse B16F1 tumor by inducing tumor-specific immune response.	39th Annual meeting of European Society for Dermatological Research (in Hungary)	September 9-12, 2009
Jimbow K, Thomas PD, Osai Y, Takada T, Sato M, Sato A, Tamura T	Melanogenesis substrate, N-propionyl cysteaminyl-phenol is selectively incorporated into melanoma cells and inhibits the growth of re-challenged secondary transplantation.	6th International Melanoma Research Congress (in USA, Boston)	November 1-4, 2009
Jimbow K, Takada T, Sato M, Sato A, Kamiya T, Ono I, Yamashita T, Tamura Y, Sato N, Miyamoto A, Wakamatsu K, Ito S, Ito A, Honda H, Murase K	Melanogenesis and nanomedicine as the basis and clinic for melanoma-targeted DDS and chemo-thermo-immunotherapy.	25th Annual Meeting of the Japanese Skin Cancer Society	May 22-23, 2009
Jimbow K, Takada T, Sato M, Sato A, Osai Y, Kamiya T, Ono I, Yamashita T, Tamura Y, Ito A, Honda H, Wakamatsu K, Ito S	Melanogenesis cascade for developing novel selective drug delivery and chemo-thermo-immunotherapeutic strategies in melanoma; specificity and biological effect.	第22回日本色素細胞学会学術大会	December 5-6, 2009
Osai Y, Tamura Y, Sato N, Wakamatsu K, Ito S, Ito A, Honda H, Okura M, Yamashita T, Jimbow K	N-propionyl-4-S-cysteaminylphenol induces apoptosis of mouse B16F1 melanoma cells and suppression of transplanted B16F1 tumors	第22回日本色素細胞学会学術大会	December 5-6, 2009
Jimbow K, Takada T, Sato M, Sato A, Osai Y, Kamiya T, Ono I, Yamashita T, Tamura Y, Ito A, Honda H, Wakamatsu K, Ito S	Utilization of melanogenesis substrate, NPrCAP for exploiting melanoma-targeting drug and its conjugation with magnetite nanoparticles for developing melanoma chemo-thermo-immunotherapy	2nd International Conference on Drug Discovery and Therapy	February 1-4, 2010

Ⅳ．研究成果の刊行物・別刷

N-Propionyl-Cysteaminylphenol-Magnetite Conjugate (NPrCAP/M) Is a Nanoparticle for the Targeted Growth Suppression of Melanoma Cells

Makito Sato[1], Toshiharu Yamashita[1], Masae Ohkura[1], Yasue Osai[1], Akiko Sato[1], Tomoaki Takada[1], Hidenobu Matsusaka[1], Ichiro Ono[1], Yasuaki Tamura[2], Noriyuki Sato[2], Yasushi Sasaki[3], Akira Ito[4], Hiroyuki Honda[5], Kazumasa Wakamatsu[6], Shosuke Ito[6] and Kowichi Jimbow[1]

A magnetite nanoparticle, NPrCAP/M, was produced for intracellular hyperthermia treatment of melanoma by conjugating N-propionyl-cysteaminylphenol (NPrCAP) with magnetite and used for the study of selective targeting and degradation of melanoma cells. NPrCAP/M, like NPrCAP, was integrated as a substrate in the oxidative reaction by mushroom tyrosinase. Melanoma, but not non-melanoma, cells incorporated larger amounts of iron than magnetite from NPrCAP/M. When mice bearing a B16F1 melanoma and a lymphoma on opposite flanks were given NPrCAP/M, iron was observed only in B16F1 melanoma cells and iron particles (NPrCAP/M) were identified within late-stage melanosomes by electron microscopy. When cells were treated with NPrCAP/M or magnetite and heated to 43°C by an external alternating magnetic field (AMF), melanoma cells were degraded 1.7- to 5.4-fold more significantly by NPrCAP/M than by magnetite. Growth of transplanted B16 melanoma was suppressed effectively by NPrCAP/M-mediated hyperthermia, suggesting a clinical application of NPrCAP/M to lesional therapy for melanoma. Finally, melanoma cells treated with NPrCAP/M plus AMF showed little sub-G1 fraction and no caspase 3 activation, suggesting that the NPrCAP/M-mediated hyperthermia induced non-apoptotic cell death. These results suggest that NPrCAP/M may be useful in targeted therapy for melanoma by inducing non-apoptotic cell death after appropriate heating by the AMF.

INTRODUCTION

Although early lesions of primary melanoma are curable by excision, successful treatment of metastatic melanoma has been elusive thus far. The current systemic therapies have little effect on the overall survival period or rate of advanced melanoma (Balch et al., 2001). Because melanogenesis is inherently toxic and uniquely expressed in melanocytic cells, tyrosine analogs can be good candidates for melanoma-

specific targeting and therapy (Jimbow et al., 1993). To develop melanocytotoxic compounds for rational chemotherapy for melanoma, N-acetyl-cysteaminylphenol and N-propionyl-cysteaminylphenol (NPrCAP) were synthesized. These compounds showed selective cytotoxicity against melanoma cells in vivo and in vitro (Jimbow et al., 1984; Miura et al., 1990; Alena et al., 1994; Tandon et al., 1998). They have both cytostatic and cytocidal effects on melanoma cells (Thomas et al., 1999), and induce apoptosis in follicular melanocytes of mice (Minamitsuji et al., 1999). Thus, these synthetic compounds would provide the basis for the development of novel anti-melanoma agents.

Iron oxide and magnetite nanoparticles are becoming versatile tools for medical imaging of lymph nodes and are excellent candidates for hyperthermia induced by an external alternating magnetic field (AMF) due to the loss of hysteresis (Leary et al., 2006; van Vlerken and Amiji, 2006). Local hyperthermia is induced in tumors by injecting magnetite nanoparticles into the core of the solid tumor and AMF irradiation results in shrinkage of animal tumors (Luderer et al., 1983; Minamimura et al., 2000). Magnetite cationic liposomes (MCL) have been generated for the selective accumulation of magnetite nanoparticles in tumor tissues,

[1]Department of Dermatology, Sapporo Medical University, Sapporo, Japan; [2]Department of 1st Pathology, Sapporo Medical University, Sapporo, Japan; [3]Department of Molecular Biology, Cancer Research Institute, Sapporo Medical University, Sapporo, Japan; [4]Department of Chemical Engineering, Faculty of Engineering, Kyushu University, Fukuoka, Japan; [5]Department of Biotechnology, Nagoya University, Nagoya, Japan and [6]Department of Chemistry, Fujita Health University, Aichi, Japan

Correspondence: Dr Toshiharu Yamashita, Department of Dermatology, Sapporo Medical University School of Medicine, South 1, West 16, Chuo-ku, Sapporo 060-8543, Japan. E-mail: yamasita@sapmed.ac.jp

and MCL-mediated hyperthermia has inhibited growth or induced complete regression of various tumors in the transplanted animals (Yanase *et al.*, 1998; Ito *et al.*, 2003; Kawai *et al.*, 2005). If the magnetite nanoparticle technology is taken a step farther to achieve a selective delivery system to tumors, guided hyperthermia could be achieved for treatment of metastatic tumors.

Recently, we synthesized an MCL in which NPrCAP was encapsulated within the liposomes, resulting in both intracellular hyperthermia and cytotoxicity when injected into animal melanoma (Ito *et al.*, 2007). Here, we introduce another magnetite nanoparticle, NPrCAP/M, to which NPrCAP was superficially bound to enhance its targeting activity to melanoma cells. The possible mechanisms of NPrCAP/M-mediated hyperthermia against melanoma are discussed.

RESULTS

Incorporation of *N*-(1-mercaptopropionyl)-4-*S*-cysteaminylphenol (NPrCAP-SH) with magnetite

The degree of incorporation of NPrCAP-SH with magnetite was determined by HCl hydrolysis of NPrCAP/M followed by HPLC analysis of the 4-*S*-cysteaminylphenol (4-*S*-CAP) produced. We measured 4-*S*-CAP as an index of the degree of NPrCAP-SH incorporation as they share the same structural units. The results indicated that the degree of incorporation of NPrCAP-SH with magnetite was 405 nmol mg^{-1} magnetite. When B16F1 cells were cultured in NPrCAP/M-containing medium, collected, and exposed to the AMF generator, the temperature rose sharply from 30 to 50°C within 10 minutes and decreased immediately after the machine was switched off (Figure 1).

NPrCAP/M as substrate for tyrosinase

We examined whether NPrCAP/M could act as a substrate for tyrosinase. 4-*S*-CAP itself was found to be a good substrate for mushroom tyrosinase; tyrosinase oxidation of 4-*S*-CAP (100 μM) in the presence of cysteine yielded 5-*S*-cysteami-nyl-3-*S'*-cysteinylcatechol through *ortho*-quinone within 10 minutes. HPLC showed that the reaction was almost completed within 10 minutes with half of the 4-*S*-CAP remaining after 4.2 minutes. At the same time, the expected catechol derivative was produced at 85 μM (85% yield) at 10 minutes. As NPrCAP/M has the same structural units as 4-*S*-CAP, it was expected to be a substrate for tyrosinase. If this were the case, 5-*S*-cysteaminyl-3-*S'*-cysteinylcatechol would be obtained by HCl hydrolysis of the cysteinylcatechol derivative of NPrCAP/M produced after tyrosinase oxidation of NPrCAP/M in the presence of cysteine. NPrCAP/M fell to half of the initial concentration after 69 minutes, and the concentration of 5-*S*-cysteaminyl-3-*S'*-cysteinylcatechol produced after 3 hours was 80 μM (80% yield) (Figure 2). Thus, the ratio of 4-*S*-CAP to NPrCAP/M in the reaction velocity on tyrosinase oxidation was 16. These results indicate that NPrCAP/M served as a substrate for mushroom tyrosinase.

Measurement of the magnetite incorporated into cells treated with NPrCAP/M

To examine whether NPrCAP/M could be incorporated into melanoma cells more preferentially than magnetite alone, we compared amounts of iron molecules in cells after culture in the NPrCAP/M- or magnetite-containing medium. To prevent non-specific adsorption of the particles to the cells, culture flasks were filled with NPrCAP/M-containing medium and rotated. After cells were collected and lysed, the amount of iron was measured. As shown in Figure 3, MM418, 70W, B16F1, SK-mel-23, TXM18, AK-1, and 96E melanoma cells incorporated large amounts of iron derived from NPrCAP/M compared with that from magnetite alone. Primary human melanocytes and non-pigmented SK-mel-24 and SK-mel-118 cells captured a relatively large amount of NPrCAP/M; however, the amount was not significantly different from that from magnetite treatment or almost the same as for magnetite (Figure 3).
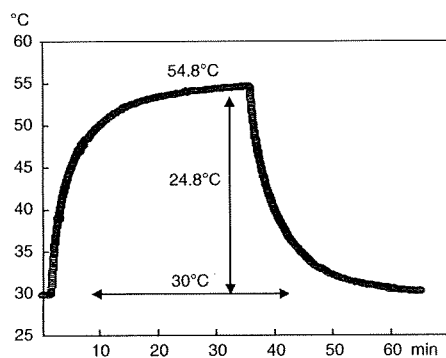

Figure 1. Heat generation in cells treated with NPrCAP/M and irradiated by AMF. 2 × 10⁶ B16F1 cells were cultured in NPrCAP/M (5.0 mg magnetite equivalent)-containing medium for 30 minutes, collected, and exposed to the center of the coil of the AMF generator. The temperature at the center of the cell pellets was measured using an optical fiber probe. A rapid increase and decrease in temperature were observed in the cell pellet during AMF irradiation.
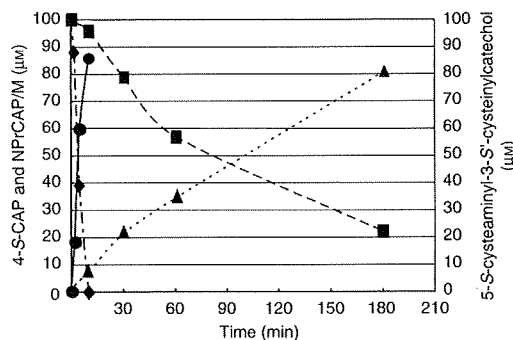

Figure 2. NPrCAP/M is incorporated into the tyrosinase oxidative reaction *in vitro*. The concentrations of the substrate remaining as 4-*S*-CAP and the 5-*S*-cysteaminyl-3-*S'*-cysteinylcatechol produced were measured by HPLC analysis after hydrolysis with HCl. ♦: 4-*S*-CAP, ■: NPrCAP/M, ●: 5-*S*-cysteaminyl-3-*S'*-cysteinylcatechol from 4-*S*-CAP, ▲: 5-*S*-cysteaminyl-3-*S'*-cysteinylcatechol from NPrCAP/M.
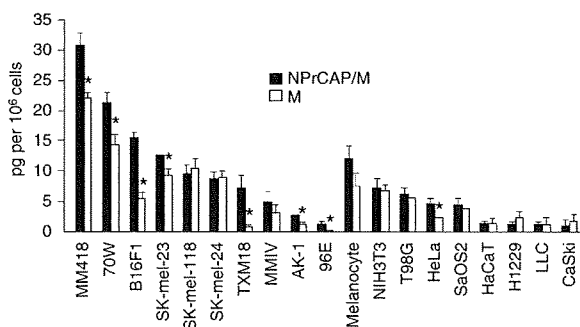
Figure 3. Uptake of magnetite nanoparticles into melanoma and non-melanoma cells. 75 cm² flasks containing growing cells were filled with NPrCAP/M- or magnetite-containing medium and fixed on a slanted disc, which was rotated slowly for 30 minutes. Incorporated iron was measured by the potassium thiocyanate method. Melanoma cell line names (MM418 to 96E) are written in gothic. Data and bars are mean ± SD of three independent experiments (*P<0.05).

NPrCAP/M is delivered to transplanted B16F1 melanomas

We then tested whether NPrCAP/M could be delivered to B16F1 melanoma tumors transplanted into syngeneic C57BL/6 mice. In five sets of experiments, each of which consisted of three to five mice, we transplanted a B16F1 melanoma onto the left flank and an EG7 or RMA lymphoma onto the right flank, and we injected NPrCAP/M or magnetite into the intraperitoneal cavity. After being allowed to grow for 2 weeks, tumors were excised and examined for the presence of iron (NPrCAP/M) by Berlin blue staining. Blue-stained cells were detected in 11 of the 14 melanomas, but in none of the 14 lymphomas (Figure 4a and b, Table 1). Meanwhile, in the B16F1- and EG7-bearing mice given magnetite, blue-stained tumor cells were not detected in either the melanoma or lymphoma tissues.

B16F1 melanomas were removed and examined for the subcellular localization of iron particles by electron microscopy. B16F1 cells in the NPrCAP/M-injected mice contained iron particles within dense ellipsoidal organelles, corresponding to late-stage melanosomes (data not shown). This suggested that NPrCAP/M was finally delivered to the melanogenesis system of the melanocytic cells.

Cytotoxic effects of magnetically mediated hyperthermia on melanoma cells

Because melanoma cells preferentially take up NPrCAP/M, it was expected that NPrCAP/M-treated melanoma cells would be selectively degraded by the AMF irradiation. MM418, SK-mel-23, B16F1, and TXM18 melanoma and H1229, HaCaT, HeLa, and SaOS2 non-melanoma cells were cultured in the NPrCAP/M- or magnetite-containing medium, collected, and irradiated by AMF at 43°C for 30 minutes. Figure 5 shows the results for NPrCAP/M- or magnetite-treated cells with or without hyperthermia induced by AMF. All the melanoma cells tested were degraded more significantly by NPrCAP/M with AMF than by magnetite with AMF, with differences ranging from 1.7-fold in SK-mel-23 to 5.4-fold in B16F1 cells (Figure 5a), whereas non-melanoma cells were degraded
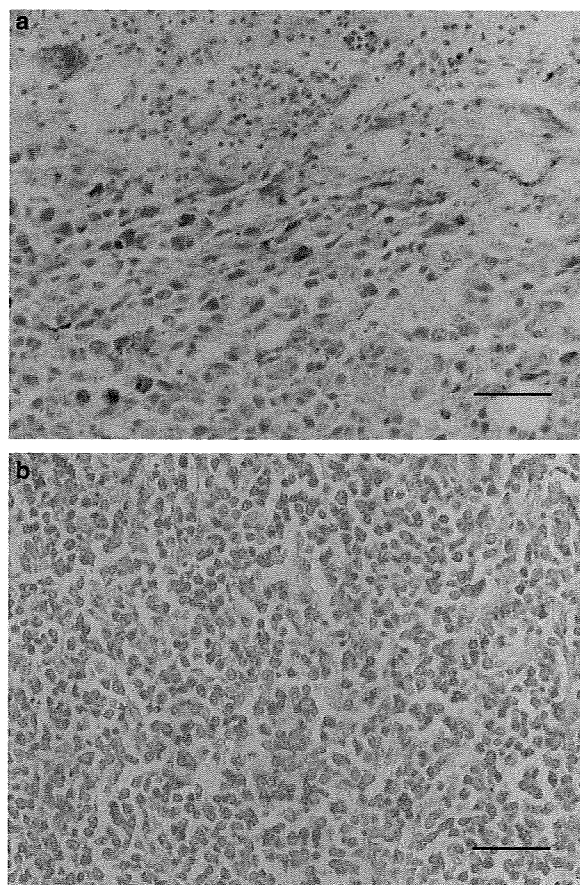

Figure 4. Intraperitoneal NPrCAP/M nanoparticles were delivered to the subcutaneously transplanted melanoma tumors. Mice bearing B16F1 and lymphoma tumors received i.p. administration of NPrCAP/M and were maintained for 14 days. Tumors were then removed and processed for hematoxylin-eosin and Berlin blue staining. Iron-containing blue-stained tumor cells were detected in the B16F1 tissues (a), but not in the EG7 (b) or RMA lymphoma tissues. Data are for five or four independent mice, each. Bars represent 50 μm (a, b).

almost equally by NPrCAP/M and magnetite (Figure 5b). These results suggested that NPrCAP/M could induce the death of melanoma cells more selectively and significantly than that of non-melanoma cells at the relatively low temperature of 43°C.

Hyperthermia mediated by NPrCAP/M effectively suppresses growth of mouse melanoma

To evaluate whether NPrCAP/M-mediated hyperthermia could suppress melanoma in the mouse model, we treated the subcutaneously transplanted B16F1 melanoma and measured the volumes of tumors (Figure 6). As shown in Figure 6a, B16F1 melanoma in mice treated by magnetite injection followed by AMF irradiation and NPrCAP/M injection followed by AMF irradiation resulted in statistically significant suppression of tumor growth compared with the untreated melanoma (Figure 6a and b). NPrCAP/M-mediated hyperthermia seemed to suppress growth of the melanoma

more than hyperthermia mediated by magnetite alone; however, differences between the two groups were not statistically significant.

Table 1. Presence of iron-containing tumor cells in mice injected with NPrCAP/M or magnetite

	Number of mice bearing a Berlin-blue positive tumor/number of total mice tested		
	B16F1	**EG7**	**RMA**
Exp I NPrCAP/M	5/5	0/5	NT
Exp II NPrCAP/M	3/4	NT	0/4
Exp III NPrCAP/M	3/5	0/5	NT
Exp IV magnetite	0/3	0/3	NT
Exp V magnetite	0/3	NT	0/3

Mice bearing B16F1 melanoma and EG7 or RMA lymphoma on the left and right flanks, respectively, were intraperitoneally given NPrCAP/M or magnetite. Tumors were excised and the presence of iron was examined by Berlin-blue staining.

Non-apoptotic cell death is induced by NPrCAP-mediated intracellular hyperthermia

Cellular DNA was prepared after cells had been cultured in the NPrCAP/M-containing medium followed by AMF at 43°C and subjected to analysis by flow cytometry. B16F1 and SK-mel-23 cells infected with a recombinant adenovirus expressing Ad-p63′ showed evident sub-G1 fractions, whereas cells subjected to NPrCAP/M-mediated hyperthermia contained little sub-G1 DNA (Figure 7). Levels of caspases 3, 8, and 9 in B16F1 and SK-mel-23 cells after NPrCAP/M-mediated hyperthermia were as low as those without NPrCAP/M or after NPrCAP/M treatment without hyperthermia (Figure 8). These results suggested that NPrCAP/M-mediated hyperthermia induced non-apoptotic cell death or necrosis.

DISCUSSION

The temperature at the center of the pellet of NPrCAP/M-treated B16F1 cells rose to over 50°C within 10 minutes; thus, the NPrCAP/M was a good heat generator, comparable to MCL or 4-S-CAP-loaded magnetite (Shinkai *et al.*, 1996;
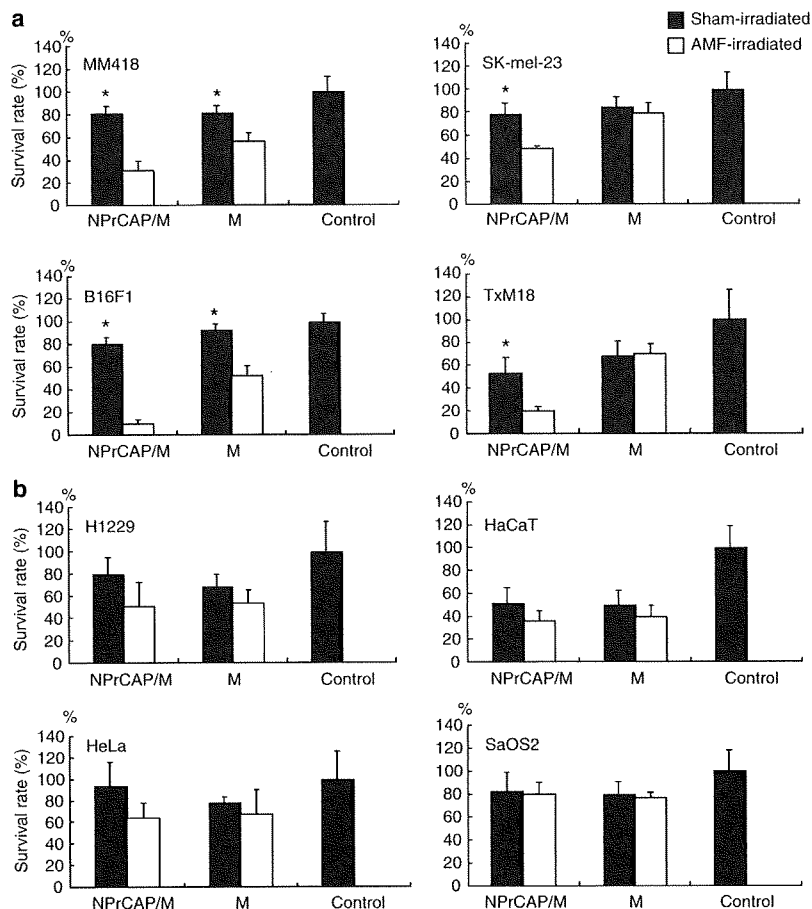

Figure 5. NPrCAP/M plus AMF treatment degraded melanoma cells more significantly than NPrCAP/M without the AMF. After cells were cultured in the NPrCAP/M-containing medium and collected, cell pellets were exposed to sham (■) or AMF (□) irradiation. Treated cells were collected and the number of viable cells not stained by trypan blue was counted. Data and bars are mean ± SD of three independent experiments (*P<0.05). (a and b) show results for melanoma and non-melanoma cell lines, respectively.
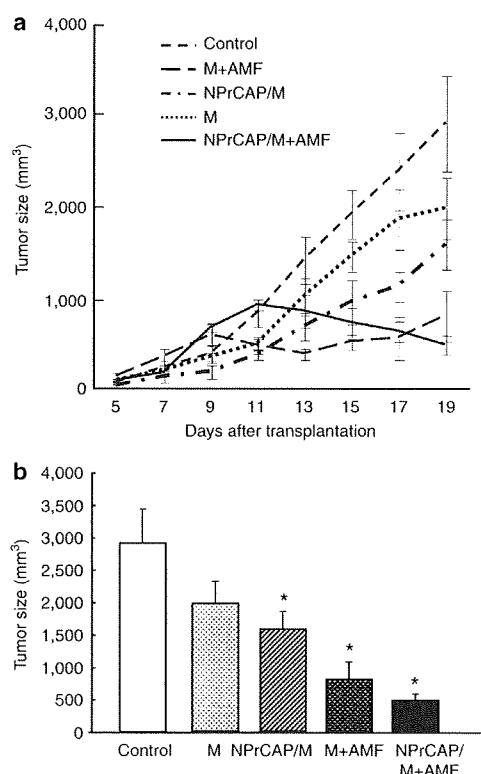
Figure 6. **Tumor volumes of the B16F1-bearing mice treated by magnetite- and NPrCAP/M-mediated hyperthermia.** (a) Comparison of groups in the first 19 days after tumor transplantation. Magnetite or NPrCAP/M (4 mg of magnetite or its equivalent) was injected directly into subcutaneous B16F1 tumors, which were then irradiated with an AMF at 46°C for 30 minutes. Each point represents the mean ± SD of five mice. All data are presented as mean ± SD. (b) Comparison of tumor volumes in each group on the 19th day. *$P < 0.005$, tumors treated by NPrCAP/M with the AMF, magnetite (M) with the AMF, and NPrCAP/M without the AMF were significantly different from those of control mice.

Figure 7. **The sub-G1 fraction was not observed in NPrCAP/M-treated and AMF exposed cells.** After cells were treated with NPrCAP/M followed by AMF irradiation and culture for 24 or 48 hours, adherent and floating cells were collected and sub-G1, G1, S, and G2/M populations were quantified with a FACScan Cell Sorter. (a): SK-mel-23 with Ad-LacZ, (b): B16F1 with LacZ, (c): SK-mel-23 with Ad-p63′, (d): B16F1 with Ad-p63′, (e): SK-mel-23 with NPrCAP/M + AMF, (f): B16F1 with NPrCAP/M + AMF.

Yanase *et al.*, 1997; Ito *et al.*, 2007). To examine NPrCAP/M as a tyrosinase substrate, we could not use the spectrophotometric assay owing to the brown suspension of the substrate. Thus, we used a method based on the fact that *ortho*-quinone obtained from tyrosinase oxidation of the substrate can be trapped with cysteine, and we monitored the cysteine adduct with HPLC. Tandon *et al.* (1998) have reported that NPrCAP is a very good substrate for tyrosinase and the enzyme's kinetic parameters (K_m and V_{max}) were found to be similar to those of the homolog N-acetyl-4-S-CAP. They also reported that the K_m values for 4-S-CAP and NPrCAP were 117 and 340 μM, whereas the V_{max} values were 39.0 and 5.4 μmol min^{-1} mg^{-1} of protein, respectively. In this study, the ratio of 4-S-CAP to NPrCAP/M in the reaction velocity on tyrosine oxidation was 16. The reaction velocity was not as good as for 4-S-CAP (Figure 2). However, it should be efficient enough, if we consider the bulky structure of NPrCAP/M.
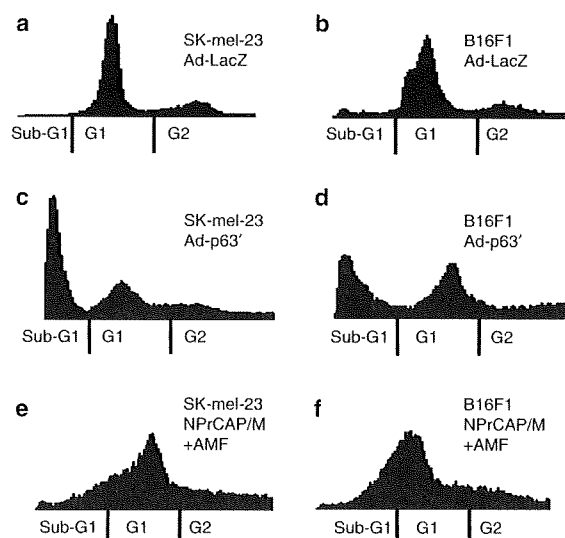
Pigmented melanoma cells, such as B16F1, MM418, 70W, and SK-mel-23, captured larger amounts of iron from NPrCAP/M than from magnetite (Figure 3). These pigmented melanoma cells also captured magnetite particles without NPrCAP, although the amount of iron from the magnetite was lower than that from NPrCAP/M. It is unclear why nonpigmented AK-1 and 96E and non-melanoma HeLa cells incorporated NPrCAP/M more efficiently than magnetite. It is possible that an unidentified receptor for cysteaminylphenols might be present on the surface or in the cytoplasm of the cells. When mice bearing B16F1 melanoma were intraperitoneally injected with NPrCAP/M, a total of 11 of 14 melanoma tissues on 14 mice contained B16F1 cells showing Berlin blue iron staining. As NPrCAP/M was injected into the peritoneal cavity in the mice, the nanoparticles were delivered to the B16 melanoma in the subcutis through the bloodstream. In the B16F1 tumors in the mice injected with magnetite, blue-stained cells were detected in the encapsulating fibroblast-like cells, but not in the tumor cells, suggesting that NPrCAP/M, but not magnetite, was preferentially delivered to the B16F1 cells. However, a large part of NPrCAP/M given i.p. was captured in reticuloendothelial cell systems such as the liver and spleen in the mice (data not shown). Clinical trials using the present magnetite-NPrCAP nanoparticles might be limited to lesional therapy against melanoma. We have proceeded to a phase I/II study of the effect of NPrCAP/M-mediated hyperthermia not only on treated tumors but also on non-treated metastatic tumors.

Hyperthermia reduces cell viability and proliferation in a time- and temperature-dependent manner in melanoma
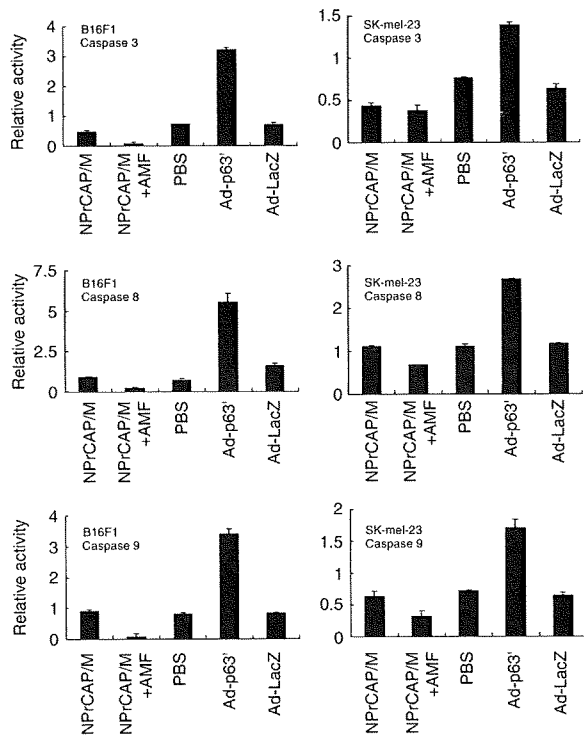
Figure 8. Caspases 3, 8, and 9 were not activated in cells that received NPrCAP/M-mediated hyperthermia. B16F1 mouse melanoma cells and SK-mel-23 human melanoma cells were treated with NPrCAP/M with or without hyperthermia. Cells were infected with 20 pfu per cell of Ad-p63' or Ad-LacZ for 24 hours for the positive control of apoptotic cell death. Cells were collected and processed for assay of caspase activities. Error bars represent the mean ± SD from two separate experiments.

cells (Shellman *et al.*, 2007). Intracellular hyperthermia of NPrCAP/M-treated cells resulted in a significant degradation of melanoma cells (Figure 5a). No difference was found in the cell numbers of non-melanoma cell lines between NPrCAP/M- and magnetite-treated dishes (Figure 5b). These results were comparable to those of an iron-incorporation assay of cells cultured in NPrCAP/M- and magnetite-containing media (Figure 3), suggesting that the targeting ability of NPrCAP/M to melanocytic cells determined the degree of cell degradation. In a previous study, significantly higher therapeutic effects were observed in mice treated with 4-*S*-CAP/MCL + AML (43°C) than in those treated with 4-*S*-CAP/MCL or hyperthermia alone (Ito *et al.*, 2007). In our animal-model experiments, growth of transplanted B16F1 tumors was suppressed more effectively than in the untreated control. Because untreated control mice died on the 19th and 21st days after inoculation, survival curves over a period of 60 days could not be compared. However, two and one mice that received NPrCAP/M- and magnetite-mediated hyperthermia survived to the 60th day after treatment, respectively, whereas mice belonging to the other groups did not. Therefore, NPrCAP/M- and magnetite-mediated hyperthermia was suggested to be more effective for tumor suppression

than treatment without heat. Interestingly, NPrCAP/M injection without heat suppressed B16 melanoma more than in the control mice (Figure 6b), suggesting that NPrCAP possessed intrinsic cytotoxicity against melanoma cells. Another experimental system that can evaluate targeting, permeating, and suppressive abilities of NPrCAP/M needs to be designed.

Necrotic, but not apoptotic, cell death is believed to induce inflammation and immunity in the host (Shellman *et al.*, 2007). When HL-60 cells were cultured at 43°C for 1 hour, cell degradation was observed in association with cellular DNA fragmentation and activation of caspases 3 and 8 (Han *et al.*, 2007). It has also been reported that hyperthermia at 41–44°C promotes TRAIL-induced apoptosis by facilitating caspase activity, whereas hyperthermia at 45–46°C inhibits this type of apoptosis (Yoo and Lee, 2007). In contrast to *in vivo* observation of apoptotic cell death of follicular melanocytes in NPrCAP-injected mice (Minamitsuji *et al.*, 1999), we found no evidence of apoptosis in cells treated with NPrCAP/M-mediated hyperthermia at 43°C. None of the caspase 8, caspase 9, or caspase 3 required for the execution of the final phase of apoptosis was activated in cells treated with NPrCAP/M and irradiated with the AMF. Although it is unclear why NPrCAP/M-mediated hyperthermia at a relatively low temperature (43°C) induced non-apoptotic cell death, this thermotherapy might elicit systemic T-cell immunity in advanced melanoma. Evidence along this line has been obtained by our group (Sato *et al.*, manuscript submitted for publication).

HSPs are molecular chaperones in the cytoplasm upregulated by various stress stimuli that damage proteins and promote accumulation of misfolded proteins (Brostrom and Brostrom, 1998). HSP70 was efficiently produced and excreted from B16F1 cells treated with NPrCAP/M and heated at 43°C compared with those heated at 46°C (data not shown). When transplanted B16F1 melanoma in mice was treated with NPrCAP/M-mediated hyperthermia at 43°C for 30 minutes, rechallenged melanoma was clearly suppressed (Takada *et al.*, manuscript submitted for publication). In this animal model system, the first tumors treated at 43°C contained larger amounts of HSP70 than those treated at 46°C. Judging from these results, HSP70 was produced most abundantly by the NPrCAP/M-mediated hyperthermia at 43°C, and the combination therapy with NPrCAP/M plus hyperthermia at this temperature resulted in the most significant therapeutic effect on advanced melanoma.

MATERIALS AND METHODS

Cell lines and cell culture

Human cancer cell lines (T98G, HeLa, SaOS2, HaCaT, H1229, and CaSki), human melanoma cell lines (SK-mel-23, SK-mel-24, SK-mel-118, MM418, 70W, TXM18, MMIV, AK-1, and 96E), murine melanoma cell line B16F1, and fibroblast cell line NIH3T3 were cultured in Dulbecco's Modified Eagle's Medium (DMEM, Gibco BRL, Gaithersburg, MD) supplemented with 5% fetal bovine serum (FBS) and antibiotics. Murine lymphoma cell lines EG7, LLC and RMA were cultured in RPMI-1640 supplemented with 5% FBS. Primary human epidermal melanocytes (BioWhittaker Inc., Walkerville, MD, USA) were grown in the basal medium supplemented

with basic FGF, hydrocortisone, TPA, insulin, and bovine pituitary extract according to the manufacturer's instructions.

Establishment of tumors in mice

Female C57BL/6 mice (age 4 weeks, weighing approximately 10.0 g) were purchased from Hokudo Co. Ltd. (Sapporo, Japan). Cell suspensions containing approximately 1×10^6 B16F1 melanoma, EG7, or RMA lymphoma cells in 0.1 ml of phosphate-buffered saline (PBS) were injected subcutaneously into C57BL/6 mice after anesthesia by diethyl ether. B16F1 melanoma and EG7 or RMA lymphoma cells were injected subcutaneously into the left and right flanks of C57BL/6 mice, respectively. Mice with tumors received intraperitoneal administration of 123.8 mg of NPrCAP/M on the third day after tumor injection. At the 15th day after transplantation, tumors were removed and processed for Fe staining. The Committees for Animal Research of Sapporo Medical University approved the experimental protocols of this research project.

Animal treatment model

Mouse B16F1 melanoma cells (5.0×10^5) in 0.1 ml of PBS were inoculated s.c. into the right flanks of 4-week-old female C57BL/6 mice. On day 5 after inoculation, mice were randomly divided into control and treatment groups. Each group was composed of five mice. With a 26-G microsyringe, the B16F1 melanoma-bearing mice were injected with 0.1 ml of NPrCAP/M or magnetite ($40.0 \, \text{mg ml}^{-1}$ solution) directly into the tumor site in a single-dose administration on days 5, 7, and 9. Hyperthermia was carried out on days 6, 8, and 10; mice were exposed to the AMF inside the coil and heated at 46°C for 30 minutes. Temperatures on the tumor surface were measured using an optical fiber probe (FX-9020; Anritsu Meter, Tokyo, Japan). Tumor size was measured every other day for 60 days by the formula: long axis × (short axis)^2 × 0.5. Data were analyzed by one- or two-way analysis of variance, and then differences in experimental results for tumor growth were assessed by Sheffe's test to compare all the experimental groups, or by Dunnett's test, which compared the experimental *versus* the control groups.

Iron oxide and chemicals

Magnetite nanoparticles (Fe_3O_4; average particle size, 10 nm) were kindly provided by Toda Kogyo (Hiroshima, Japan). 4-S-CAP was prepared as described by Padgette *et al.* N-succinimidyl-3-[2-pyridyldithio] propionate and mushroom tyrosinase (6050 U mg^{-1}) were obtained from Molecular Biosciences, Inc. (Boulder, CO) and Sigma Chemical Co. (St Louis, MO), respectively. 3-Aminopropyl-triethoxysilane and N-[γ-maleimidobutyryloxy]sulfosuccinimide ester were products of Tokyo Chemical Industry (Tokyo, Japan) and Pierce (Rockford, IL), respectively. All other chemicals were of analytical grade.

Synthesis of *N*-(1-mercaptopropionyl)-4-*S*-cysteaminylphenol (NPrCAP-SH)

A mixture of 1.81 g of 4-S-CAP (10.7 mmol) and 4.13 g of N-succinimidyl-3-[2-pyridyldithio] propionate (13.2 mmol) in 5 ml of pyridine was stirred for 2 hours at room temperature. After evaporation, the residue was purified by silica gel column chromatography (ethyl acetate:n-hexane; 2:1 v/v as eluant) to give a disulfide (3.70 g; 94%). Then 4.29 g of dithiothreitol (27.5 mmol) was added to a stirred solution of the disulfide (3.70 g; 10.3 mmol) in

5 ml of methanol at room temperature. After 2 hours the mixture was evaporated and the oily residue was purified by silica gel column chromatography (ethyl acetate:n-hexane; 2:1 v/v) to give 2.19 g of NPrCAP-SH (80%) as a colorless crystal after recrystallization (ethyl acetate ether). The elemental analysis of NPrCAP-SH was as follows: Anal. Calcd for $C_{11}H_{15}N_1O_2S_2$: C, 51.36; H, 5.84; N, 5.45; S, 24.90; Found: C, 51.41; H, 5.78: N, 5.50; S, 24.83. The resulting material was subjected to liquid chromatography/mass spectrometry/mass spectrometry (LC/MS/MS) analysis using an electrospray ionization/ion trap mass spectrometer (LCQ Deca XP, Thermoelectron, Tokyo, Japan). The analysis was carried out directly by MS/MS at a positive charge; $[M + H]^+$: *m/z* 258, 164, 153, 132, 125. ^{1}H NMR was measured at 400 MHz (CD_3COCD_3): 2.45 p.p.m. (2H, t, $J = 6.8$ Hz), 2.71 p.p.m. (2H, m), 2.88 p.p.m. (2H, t, $J = 6.3$ Hz), 3.32 p.p.m. (2H, m), 6.68 p.p.m. (2H, d, $J = 8.0$ Hz), 7.31 p.p.m. (2H, d, $J = 8.0$ Hz).

Conjugation of NPrCAP-SH with magnetite

To prepare the aminosilane-coated magnetite nanoparticles, 10 ml (concentration, $40 \, \text{mg ml}^{-1}$) of magnetite nanoparticles and 0.1 ml of 3-aminopropyltriethoxysilane were mixed and incubated for 1 hour with stirring at room temperature. The resultant magnetic suspension was then washed three times with 10 mM phosphate buffer (pH 6.8) by centrifugation at 2,500 r.p.m. for 2 minutes and resuspended in 10 ml of phosphate buffer. For conjugation of maleimide cross-linkers, the magnetite suspension was mixed with 200 ml of N-[γ-maleimidobutyryloxy]sulfosuccinimide ester ($10 \, \text{mg ml}^{-1}$), and incubated in PBS for 30 minutes with shaking at room temperature. The resultant magnetite suspension was washed three times with water by centrifugation at 2,500 r.p.m. for 2 minutes. Then 0.5 ml of NPrCAP-SH ($50.0 \, \text{mg ml}^{-1}$ of ethanol) was added to 10 ml of the magnetite suspension ($40.0 \, \text{mg ml}^{-1}$) and the mixture was stirred for 30 minutes at room temperature. After standing for 2 hours at room temperature, the suspension was washed twice with water by centrifugation at 3,000 r.p.m. for 1 minute. The resultant NPrCAP/M was resuspended in Milli-Q water to a concentration of $40 \, \text{mg ml}^{-1}$.

Analysis of NPrCAP incorporated with magnetite nanoparticles

The degree of incorporation of NPrCAP-SH with magnetite was determined by hydrolysis with 6 M HCl followed by HPLC analysis of the resultant 4-S-CAP. Briefly, the amount of 4-S-CAP produced by the hydrolysis of NPrCAP/M with 6 M HCl at 110°C for 1.5 hours was measured by HPLC using a Jasco PU-980 Intelligent liquid chromatogram with a Jasco 851-AS Intelligent autosampler (JASCO, Tokyo, Japan), a Jasco 875-UV/VIS detector, and Shiseido C18 reverse-phase column (Capcell Pak C18, 4.6 × 250 mm; 5.0 μm particle size). The UV detector was set at 250 nm. The mobile phase used was methanol:H_2O:1.0 M $HClO_4$, 10:90:1.5 by volume. The analyses were performed at 50°C at a flow rate of 0.7 ml minute^{-1}. The concentration of iron, which formed a red complex with thiocyanate, was quantitated by absorbance at 480 nm (Owen and Sykes, 1984).

Tyrosinase oxidation of NPrCAP/M

Mushroom tyrosinase (80 μg) was added to a reaction mixture containing 100 μM NPrCAP/M and 200 μM cysteine in 1 ml of 50 mM sodium phosphate buffer (pH 6.8), and oxidation was carried out at 37°C. At 30 minutes, 1 hour, and 3 hours, a 100-μl aliquot of the reaction mixture was removed and mixed with 900 μl of 0.4 M

$HClO_4$. The concentrations of the substrate remaining as 4-*S*-CAP and 5-*S*-cysteaminyl-3-*S'*-cysteinylcatechol produced were measured by hydrolysis with 6 M HCl followed by HPLC analysis (see above section, Analysis of NPrCAP incorporated with magnetic particles). The retention times of 4-*S*-CAP and 5-*S*-cysteaminyl-3-*S'*-cysteinylcatechol were 14.4 and 7.9 minutes, respectively.

Measurement of iron in the NPrCAP/M-exposed cells

Subconfluently growing melanoma and non-melanoma cells $(8 \times 10^4 cm^{-2})$ in a $25 cm^2$ flask were refed with the medium containing 5.94 mg of NPrCAP/M or magnetite (84 μg ml^{-1}). To discriminate between incorporation of NPrCAP/M by direct attachment to cells and that by diffusion from the medium, culture flasks were fixed on a slanted disc (60°) and rotated slowly for 30 minutes. After the cells were washed with PBS twice and collected, they were dissolved completely in 200 μl of concentrated HCl and incubated at 43°C for 30 minutes. Then, 10 μl of H_2O_2 and 4 ml of 1% potassium thiocyanate were added in sequence to the cell solution. The iron concentration of magnetite nanoparticles was measured using the potassium thiocyanate method as described above.

Cytotoxicity of NPrCAP/M in combination with AMF irradiation

For cytotoxicity measurement, 5×10^6 B16F1, MM418, SK-mel-23, TXM18, H1229, HaCaT, HeLa, and SaOS2 cells were cultured in the medium containing 5.94 mg of NPrCAP/M or magnetite (1.19 mg ml^{-1}) for 20 minutes. Then, the cells were harvested by centrifugation at 400 g for 10 minutes and the cell pellets were subjected to AMF irradiation at 43°C for 30 minutes. The AMF was generated by using a horizontal coil (inner diameter 7 cm, length 7 cm) with a transistor inverter (LTD-100-05; Dai-ichi High Frequency Co., Tokyo). The magnetic field frequency and intensity were 118 kHz and 30.6 kA/M (384 Oe), respectively. Cell temperatures were measured and monitored using an optical fiber probe (Anritsu Meter, Tokyo, Japan). After AMF irradiation, aliquots (1/10) of cells were seeded in a dish and cultured for a further 48 hours. Viable cells were counted using a hemocytometer.

Recombinant adenoviruses

Propagation, plaque formation, and inoculation of recombinant adenoviruses were described elsewhere (Yamano *et al.*, 1999). Ad-LacZ is a replication-deficient recombinant adenovirus carrying β-galactosidase. Ad-p63' is a recombinant adenovirus expressing modified p63, which was provided by T Tokino (manuscript in preparation and personal communication). The construction of the original adenovirus Ad-p63 containing the human p63 gene was described previously (Sasaki *et al.*, 2001, 2003). Cells were infected with 20 plaque-forming units of a recombinant adenovirus, incubated for 60 minutes at 37°C, and cultured in fresh DMEM with 5% FBS for 48 hours before flow cytometric analysis or caspase assay.

Flow cytometric analysis

After B16F1 and SK-mel-23 cells were cultured in the NPrCAP/M-containing medium (4.6 mg ml^{-1}) for 30 minutes, they were subjected to AMF irradiation at 43°C for 30 minutes, reseeded in the medium, and cultured for 24 hours. Then adherent and floating cells were collected together and washed in ice-cold PBS. The cells were dehydrated in 75% cold ethanol and stored on ice for 2 hours. Then

they were rehydrated in cold PBS and incubated in the presence of RNaseA (50 μg ml^{-1}) (Sigma Aldrich Japan, Tokyo, Japan) at 37°C for 30 minutes. After incubation, the cells were rinsed twice in ice-cold PBS and suspended in 2.0 ml of PBS containing 50 μg ml^{-1} propidium iodide (Sigma Aldrich Japan) at 4°C for 2 hours. Cell debris and fixation artifacts were gated out, and sub-G1, G1, S, and G2/M populations were quantified with a FACScan Cell Sorter (Nippon Becton Dickinson, Tokyo, Japan) using the CELL QUEST program.

Caspase enzyme assay

After 5×10^6 B16F1 and SK-mel-23 cells were collected in 15 ml tubes, 5.94 mg of NPrCAP/M was separately added to the cell pellets, which were then incubated for 20 minutes at 37°C in a CO_2 incubator. Cells were harvested by centrifugation at 400 g for 10 minutes and irradiated by the AMF as described above. Cells were then collected and seeded in 10 cm dishes and cultured for a further 24 hours. Both the floating and the adherent cells were collected, washed with PBS, and processed for caspase assay. Activities of caspases 3, 8, and 9 were measured using a colorimetric protease kit according to the manufacturer's protocol (MBL, Nagoya, Japan).

CONFLICT OF INTEREST
The authors state no conflict of interest.

REFERENCES

Alena F, Iwashina T, Gili A, Jimbow K (1994) Selective *in vivo* accumulation of *N*-acetyl-4-*S*-cysteaminylphenol in B16F10 murine melanoma and enhancement of its *in vitro* and *in vivo* antimelanoma effect by combination of buthionine sulfoximine. *Cancer Res* 54:2661-6

Balch CM, Buzaid AC, Soong S-J, Atkins MB, Cascinelli N, Coit DG *et al.* (2001) Final version of the American Joint Committee on Cancer staging system for cutaneous melanoma. *J Clin Oncol* 19:3635-48

Brostrom CO, Brostrom MA (1998) Regulation of translational initiation during cellular responses to stress. *Prog Nucleic Acid Res Mol Biol* 58:79-125

Han Q-S, Yumita N, Nishigaki R (2007) Involvement of caspases 3, 8,and 9 signaling pathways in hyperthermia induced apoptosis in HL-60 cells. *Thermal Med* 23:31-40

Ito A, Fujioka M, Yoshida T, Wakamatsu K, Ito S, Yamashita T *et al.* (2007) 4-*S*-cysteaminylphenol-loaded magnetite cationic liposomes for combination therapy of hyperthermia with chemotherapy against malignant melanoma. *Cancer Sci* 98:424-30

Ito A, Tanaka K, Kondo K, Shinkai M, Honda H, Matsumoto K *et al.* (2003) Tumor regression by combined immunotherapy and hyperthermia using magnetic nanoparticles in an experimental subcutaneous murine melanoma. *Cancer Sci* 94:308-13

Jimbow K, Iwashina T, Alena F, Yamada K, Pankovich J, Umemura T (1993) Exploitation of pigment biosynthesis pathway as a selective chemotherapeutic approach for malignant melanoma. *J Invest Dermatol* 100:S231-8

Jimbow K, Miura S, Ito Y, Kasuga T, Ito S (1984) Utilization of melanin precursors for experimental chemotherapy of malignant melanoma. *Jpn J Cancer Chemother* 11:2125–32

Kawai N, Ito A, Nakahara Y, Futakuchi M, Shirai T, Honda H *et al.* (2005) Anticancer effect of hyperthermia on prostate cancer mediated by magnetite cationic liposomes and immune-response induction in transplanted syngeneic rats. *Prostate* 64:373–81

Leary SP, Liu CY, Apuzzo ML (2006) Toward the emergence of nanoneurosurgery: part II-nanomedicine: diagnostics and imaging at nanoscale level. *Neurosurgery* 58:805–23

Luderer AA, Borrelli NF, Panzario JN, Mansfield GR, Hess DM, Brown JL *et al.* (1983) Glass-ceramic-mediated, magnetic-field-induced localized hyperthermia: response of a murine mammary carcinoma. *Radiat Res* 94:190–8

Minamimura T, Sato H, Kasaoka S, Saito T, Ishikawa S, Takemori S *et al.* (2000) Tumor regression by inductive hyperthermia combined with hepatic embolization using dextran magnetite-incorporated microspheres in rats. *Int J Oncol* 16:1153–8

Minamitsuji Y, Toyofuku K, Sugiyama S, Yamada K, Jimbow K (1999) Sulfur containing tyrosine analogs can cause selective melanocytotoxicity involving tyrosinase-mediated apoptosis. *J Invest Dermatol Symp Proc* 4:130–6

Miura T, Jimbow K, Ito S (1990) The *in vivo* antimelanoma effect of 4-S-cysteaminylphenol and its N-acetyl derivative. *Int J Cancer* 46:931–4

Owen CS, Sykes NL (1984) Magnetic labeling and cell sorting. *J Immunol Methods* 73:41–8

Padgette SR, Herman HH, Han JH, Pollock SH, May SW (1984) Antihypertensive activities of phenyl aminoethyl sulfides, a class of synthetic substrates for dopamine beta-hydroxylase. *J Med Chem* 27:1354–7

Sasaki Y, Mita H, Toyota M, Ishida S, Morimoto I, Yamashita T *et al.* (2003) Identification of the interleukin 4 receptor alpha gene as a direct target for p73. *Cancer Res* 23:8145–52

Sasaki Y, Morimoto I, Ishida S, Yamashita T, Imai K, Tokino T (2001) Adenovirus- mediated transfer of the p53 family genes, p73 and p51/p63

induces cell cycle arrest and apoptosis in colorectal cancer cell lines: potential application to gene therapy of colorectal cancer. *Gene Ther* 8:1401–8

Shellman YG, Howe WR, Miller LA, Goldstein NB, Pacheco TR, Mahajan RL *et al.* (2008) Hyperthermia induces endoplasmic reticulum-mediated apoptosis in melanoma and non-melanoma skin cancer cells. *J Invest Dermatol* 128:949–56

Shinkai M, Yanase M, Honda H, Wakabayashi T, Yoshida J, Kobayashi T (1996) Intracellular hyperthermia for cancer using magnetite cationic liposomes: *in vitro* study. *Jpn J Cancer Res* 87:1179–83

Tandon M, Thomas PD, Shokravi M, Singh S, Samra S, Chang D *et al.* (1998) Synthesis and antitumour effect of the melanogenesis-based antimelanoma agent, N-propionyl-4-S-cysteaminylphenol. *Biochem Pharmacol* 55:2023–9

Thomas PD, Kishi H, Cao H, Ota M, Yamashita T, Singh S *et al.* (1999) Selective incorporation and specific cytocidal effect as the cellular basis for the antimelanoma action of sulphur containing tyrosine analogs. *J Invest Dermatol* 113:928–34

Van Vlerken LE, Amiji MM (2006) Multi-functional polymeric nanoparticles for tumour-targeted drug delivery. *Expert Opin Drug Deliv* 3:205–16

Yamano S, Tokino T, Yasuda M, Kaneuchi M, Takahashi M, Niitsu Y *et al.* (1999) Induction of transformation and p53-dependent apoptosis by adenovirus type 5 E4orf6/7 cDNA. *J Virol* 73:10095–103

Yanase M, Shinkai M, Honda H, Wakabayashi T, Yoshida J, Kobayashi T (1997) Intracellular hyperthermia for cancer using magnetite cationic liposomes: *ex vivo* study. *Jpn J Cancer Res* 88:630–2

Yanase M, Shinkai M, Honda H, Wakabayashi T, Yoshida J, Kobayashi T (1998) Intracellular hyperthermia for cancer using magnetite cationic liposomes: an *in vivo* study. *Jpn J Cancer Res* 89:463–9

Yoo J, Lee YJ (2007) Effect of hyperthermia on TRAIL-induced apoptotic death in human colon cancer cells: development of a novel strategy for regional therapy. *J Cell Biochem* 101:619–30

Epidermal melanin unit and aging of skin ; biological and molecular significance of pheomelanin in constitutive photo-aging process

[1]Kowichi Jimbow, MD, PhD, FRCPC,

[2]Takafumi Kamiya, MD, PhD and [2]Tokimasa Hida, MD, PhD

[1]Institute of Dermatology & Cutaneous Sciences, Sapporo, Japan

[2]Department of Dermatology, Sapporo Medical University School of Medicine, Sapporo, Japan

Abstract

This report describes some aspects of current progress in biological and molecular involvement of melanin pigmentation in aging process of the skin. Two types of melanin pigments are present in the skin, eumelanin and pheomelanin. The importance of re-visiting the concept of epidermal melanin unit (EMU) was introduced for better understanding the role of melanin pigmentation in aging process of the skin. We then discussed what regulates in 1) biological and molecular process of melanin pigmentation in constitutive, intrinsic aging and 2) pheomelanin biosynthesis and its involvement in facultative, extrinsic aging. The former topic was further extended into a) melanogenesis and oxidative stress in EMU after exposure to UVR,b) tyrosinase and LAMP (lysosome-associated membrane protein) gene families and oxidative stress, c) function and mutation of LAMP and TYRP (tyrosinase-related protein). The latter was extended into a) high content of pheomelanin in melanoma and its precursors, b) UV photoproducts of melanin pigmentation and cytotoxicity and c) UV-photoproducts of pheomelanin in aging process. It was indicated that, while the major role of eumelanin is to provide protection against UV-induced DNA damage by absorbing and scattering UVR, pheomelanin and its precursors are photo-chemically unstable in the presence of UVR and that their oxidation products produce short-lived singlet oxygen and its conversion to hydroxyl radicals, thus affecting significantly in constitutive aging process of the skin.

Keywords : Melanin pigmentation, aging process of skin, Eumelanin, Pheomelanin, Epidermal melanin unit, Facultative pigmentation, Constitutive pigmentation.

Introduction ; Epidermal melanin unit (EMU) and melanin pigmentation in facultative and constitutive aging processes of skin

The major determinant of the skin pigmentation in humans is the epidermal melanin unit (EMU). The EMU is composed of the orderly interaction of a melanocyte and an associated pool of keratinocytes with four major biological and biochemical processes, i.e., the synthesis and melanization of melanosomes within the melanocyte, their transfer from the tip of melanocytic dendrites to surrounding keratinocytes and their degradation within keratinocytes and exfoliation from them. If there is any alteration of these processes, hypo- or hyperpigmentation occurs and results in various skin pigmentation ranging from white, light brown, brown to black skin. If there is, however, any dropping off of melanosomes into the dermis or any growth of dermal melanocytes, slate blue or blue pigmentation occurs[25].

There will be the increase of skin pigmentation with natural aging of the skin and this will be typically seen in darkening of the skin in aged Orientals such as in Japanese. The increased melanin pigmentation after exposure to UVR may damage the skin and enhance the acquired skin aging as there will be increased production of free radicals during melanin formation process after exposure to UVR. The major goal of skin protection from aging process of the skin in terms of melanin pigmentation would be to repair facultative, acquired skin pigmentation, i.e.,"tanning", and to reach constitutive pigmentation, i.e., the inborn skin pigmentation. If we introduce the concept of the EMU in identifying

Correspondence to

Kowichi Jimbow, MD, PhD, FRCPC

Institute of Dermatology & Cutaneous Sciences

1-27, Odori W-17, Chuoku, Sapporo, Japan 0600042

T E L : 011-887-8266

F A X : 011-618-1213

E-mail : jimbow@sapmed.ac.jp

the methods to improve the darkening of the skin with aging, target molecules responsible for this goal may be divided into three biological and biochemical steps of pigmentation in the EMU, i.e., step 1 : exfoliation of melanin/melanosome from horny layer, step 2 : transfer of melanin and melanosomes from the melanocyte and their degradation within keratinocytes and finally step 3 : their biosynthesis within the melanocyte (Table I).

UV irradiation, in particular UVB, is directly absorbed by cellular DNA, leading to the formation of DNA photoproducts, mainly thymidine dimmers and pyrimidine (6-4) pyrimidone. Importantly the action spectrum for tanning is virtually the same as that for the formation of thymine dimmers,[14,42] and UV induced melanogenesis can be augmented in melanocytes by treatment with T4 endonuclease V, an enzyme that acts to enhance the repair of UV-induced DNA damage[13,41]. Furthermore, the tumor suppressor protein p53, when activated, up-regulates the level of tyrosinase mRNA and protein, enhancing melanogenesis[33]. Cui et al[10]. found a p53 consensus sequence in the proopiomelanocortin (POMC) gene promoter and established a continuous signaling pathway from UV-induced DNA injury to the final tanning response. It was shown that, following UVR in mice, p53 activation stimulates transcription from the POMC promoter in keratinocytes, thereby increasing the release of POMC-derived αMSH. Keratinocyte-derived αMSH then stimulates the melanocortin-1 receptor (MC 1 R) on melanocytes, resulting in increased production of black melanin. In contrast, p53 knockout control mice did not show POMC upregulation, increased αMSH, and subsequent UV-induced tanning[11].

Mammalian melanin has been divided into two major groups, i.e., eumelanin and pheomelanin[29]. Eumelanin, brown or black, is intractably insoluble and nitrogenous. It is derived from conversion of tyrosine to form dopa and dopaquinone in the presence of tyrosinase. It is basically composed of indole-quinone units which form eumelanin by either auto-oxidation or enzymic action of tyrosinase-related proteins (TYRPs). In contrast pheomelanin is formed by the nucleophilic addition of cysteine to dopaquinone, resulting in the formation of cysteinyldopas, which are then auto-oxidized to form benzothiazine units and subsequently pheomelanin. Thus synthesis of both eumelanin and pheomelanin starts from tyrosine oxidation catalyzed by tyrosinase. The resulting dopaquinone can be a precursor for either eumelanin synthesis promoted by TYRP 1 and TYRP 2 (dopachrome tautomerase ; DCT), or pheomelanin in the presence of high cysteine concentrations and low tyrosinase[25]. Eumelanin is the major component of the EMU, and only a small amount of pheomelanin is present in normal skin. Since both eumelanosomes and pheomelanosomes can be synthesized by a single melanocyte at the same time, it is expected that both eumelanin and pheomelanin are present in normal skin (Fig. 1 and 2)[23].

The mechanism of melanin synthesis and its regulation has been extensively studied by genetic studies of coat color in mice (Fig. 3 and 4)[6]. Two major loci are central to pigment-type switching (eumelanin vs pheomelanin). One is the agouti locus encoding agouti signal protein (ASIP) and other is the melanocortin-1 receptor (Mc 1 r) locus[3] MC 1 R (Mc 1 r) is a cell-

Table I : Molecular targets for skin pigmentation and anti-aging

Step 1 : Melanin/ melanosome exfoliation
    Approach 1 : Remove horny layer cells
    Approach 2 : Increase epidermal turnover
    Approach 3 : Increase the contents of water/ sebum
Step 2 : Melanin/ melanosome transfer and degradation
    Approach 1 : Melanosome degradation in keratinocytes
    Approach 2 : Melanosome transfer in melanocytes
Step 3 : Melanin/ melanosome biosynthesis
    Approach 1 : Transcription factors and MSH
    Approach 2 : Tyrosinase glycosylation and molecular chaperon
    Approach 3 : Vesicular transport of tyrosinase and melanization

surface G-protein-coupled receptor for which the best-known agonist is the soluble peptide αMSH, cleaved from the precursor POMC in the pituitary and skin[12]. Binding of αMSH to MC 1 R is known to activate adenylate cyclase and cAMP synthesis, promoting eumelanin synthesis through both post-translational[5] and transcriptional pathways via microphthalmia-associated transcription factor (MITF)[7],[35]. MITF is a master regulator for eumelanogenesis, melanocyte differentiation, proliferation and survival. It promotes transcription of melanocyte-specific gene products including melanosomal enzymes, tyrosinase, TYRP 1 and DCT and the matrix protein, i.e., SIVL/PMEL[35]. ASIP competitively antagonizes αMSH at the MC 1 R and inhibits the
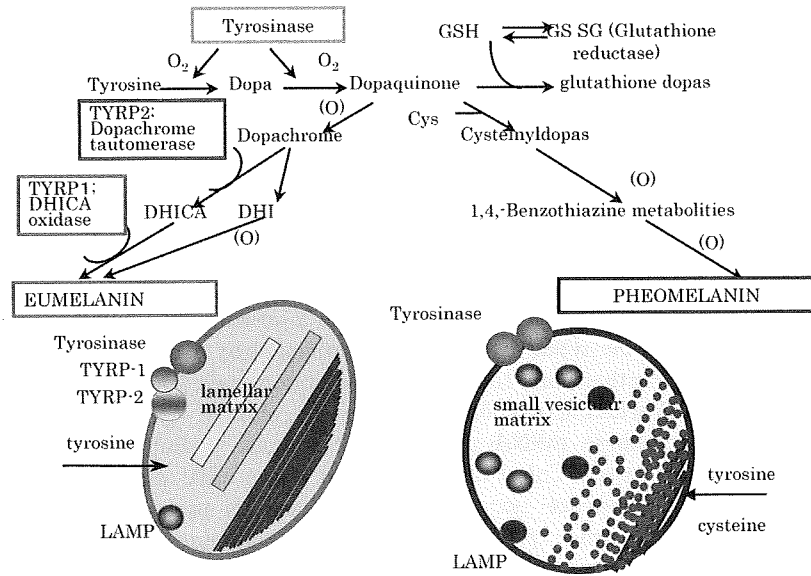

Figure 1 : Chemical and biochemical pathway for synthesis of eumelanin and pheomelanin
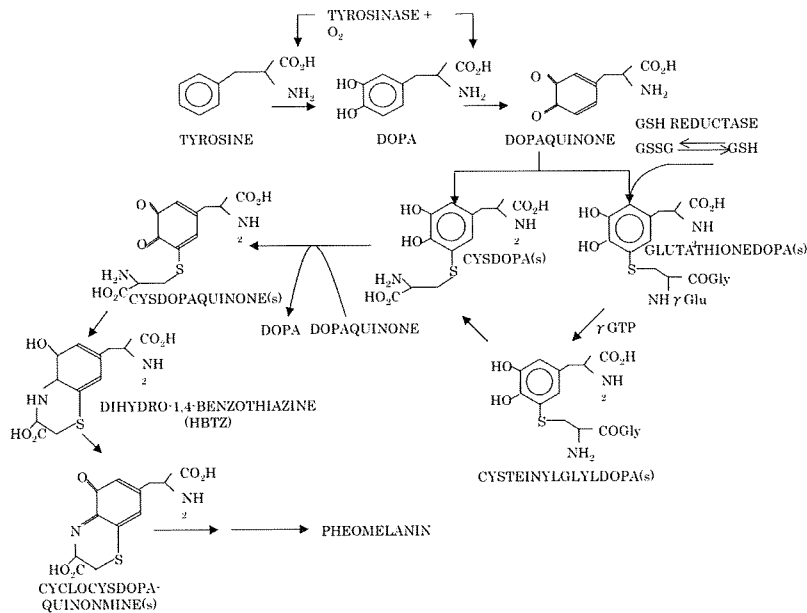

Figure 2 : Chemical reactions of pheomelanin biosynthesis. Metabolic and chemical reactions of pheomelanin synthesis

Table Ⅱ : Genetic association of MC1R variants and phenotypes in pheomelanic red hair and skin cancers

MC1R Variant	Frequency in Austrarians (%)	Red Hair		SCC/ BCC	MM	
		Smith R et al. (1998)	Kenned C et al. (2001)	Box NF et al. (2001)	Palmer JS et al. (2000)	Matichar E et al. (2004)
Val60Leu	12.4	NA	OR = 2.3	OR = 1.4	OR = 1.3	p < 0.0001 OR = 3.99
Asp84Glu	1.1	—	OR = 5.1		OR = 0.8	p = 0.41 OR = 2.16
Val92Met	9.7	NA	NA	OR = 2.1		
Arg142His	0.9		OR = 49.2			p = 0.07
Arg151Cys	11.1	p = 0.0015	OR = 20.7	OR = 2.6	OR = 2.1	p = 0.0002 OR = 6.48
Arg160Trp	7.1	p < 0.001	OR = 12.5	OR = 3.4	OR = 1.9	p = 0.0013 OR = 4.73
Arg163Gln	5.0	—	NA	OR = 1.7		
Asp294His	2.8	p < 0.005	OR = 15.0	OR = 15.0	OR = 2.3	p = 0.058 OR = 3.84

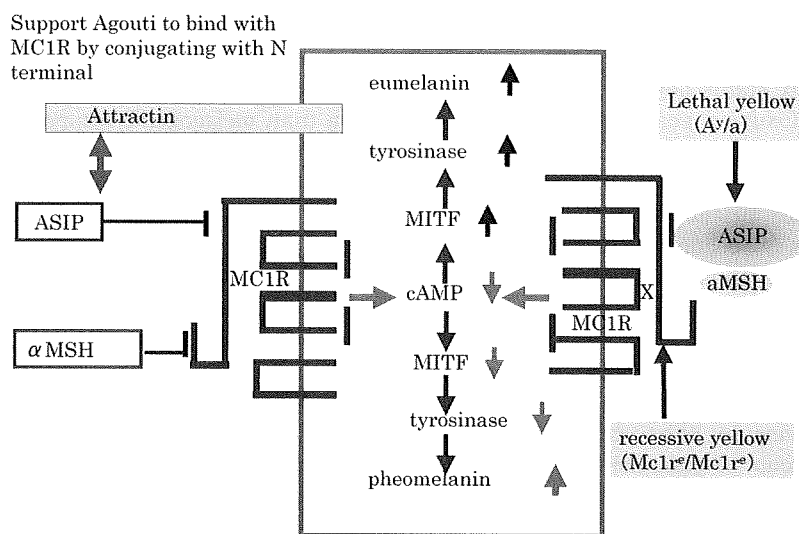SCC ; Squamous cell carcinoma, BCC ; Basal cell carcinoma, NA ; No association

Figure 3 : The interaction of ASIP and αMSH for biosynthesis of eumelanin and pheomelanin

eumelanogenic signal, down-regulating melanogenic enzymes and leading pheomelanin synthesis (Fig. 3)[39]. Polymorphisms within the MC 1 R gene are largely responsible for the wide range of skin and hair color among different ethnic groups[15]. At least 68 MC 1 R variants have been identified in humans, and several of them in fair-skinned subjects with red hair are highly associated with skin cancers and melanoma (Table Ⅱ)[41].

Eumelanin biosynthesis in EMU and aging of skin

1. Melanogenesis and oxidative stress in EMU after exposure to UVR

Alterations of the EMU in response to exposure to intrinsic and extrinsic factors are often linked to oxidative stress that produces
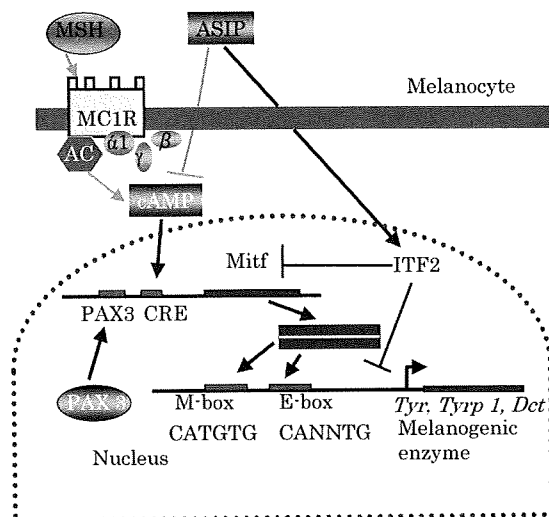
Figure 4 : Involvement of ITF 2 in transcriptional regulation for switch between eumelanin and pheomelanin biosynthesis. The figure was modified from Furumura M et al (Furumura M et al, J Biol Chem 276 : 28147–28154, 2001)
1. ITF 2 ; ubiquitous basic helix–loop–helix transcription factor (bHLP)
2. Up–regulation of ITF 2 suppresses melanogenic gene expression and Mitf expression
3. Agouti signal protein (ASIP) antagonizes the binding of MSH to MC 1 R

imbalanced redox status beyond the protective capacities of detoxifying enzymes. Melanocytes can produce such cytotoxic products during bio-synthesis of melanin pigments in the presence of tyrosinase. This melanin biosynthesis process involves a series of reactions consisting of one–electron transfer system from electron donors (phenol/ catechol amines) to electron accep-tors (quinones/ quinine amines), therefore the whole process resolves for the production of "free radicals". Quinones can be toxic at least by two mechanisms, i.e., either directly reacting with the–SH group of essential cellular mole-cules, or creating oxidative stress by redox cy-cling which results in superoxide radical ($O_2-\cdot$) and hydrogen peroxide. Quinones undergo one–electron reduction by cellular redox system to semiquinones, which are then re–oxidized by O_2 to quinine and $O_2-\cdot$. Semiquinone radicals can also be produced in the melanogenic pathway non–enzymically, through mechanisms involv-ing : a) disproportion of quinine and hydroqui-none forms of reactants (catechols and hy-droxyindoles) ;b) oxidation of catechol (amine) s by superoxide ; and c) metal ion (iron, cop-per) –catalyzed oxidation of catechol (amine) s by oxygen (Fig. 5). In addition, UV light/or

physical injury can stimulate semiquinone for-mation from melanogenic compounds via direct interaction (causing photo–ionization and/or photo–homolysis of phenolic OH groups in catechol amines and hydroxyindoles), or indi-rectly, through photosensitization (e.g., as in UV –B/ psoralen and UVA [PUVA]. These proc-esses are partly responsible for the UV light–stimulated cytotoxicity[45].

2 . Tyrosinase and LAMP gene families and oxi-dative stress

Besides tyrosinase, as discussed briefly in the above section, two molecules are related to tyrosinase and are referred to as tyrosinase-re-lated proteins (TYRPs in humans and Tyrps in animals) ; (a) TYRP 1, which is relevant to brown locus protein in mice and (b) TYRP 2, which is also present in melanosomes and has a dopachrome tautomerase (DCT) activity . These three enzymes are called tyrosinase gene family because of the structural homology among them and the identification of respective genes in the same melanocyte cDNA expression library by anti–tyrosinase antibody immuno-screening. Melanosomes and lysosomes share many common structural similarities. We and
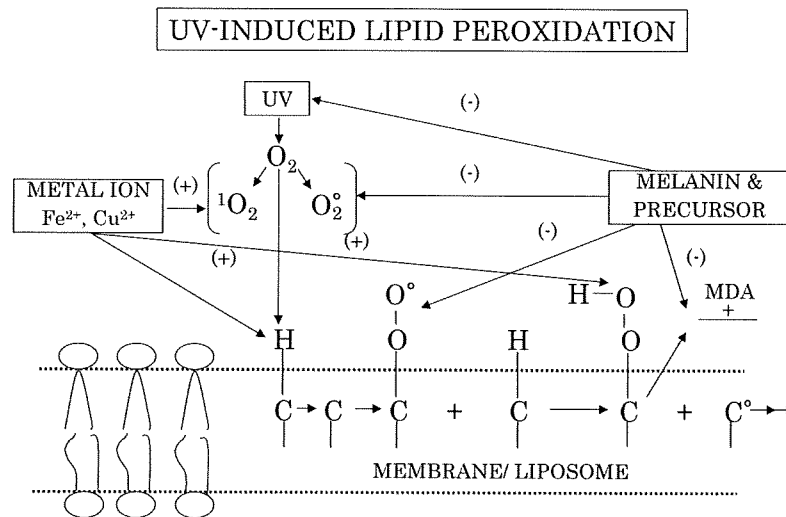
UV-INDUCED LIPID PEROXIDATION

Figure 5 : UV-induced cell damage by lipid peroxidation of the cell membrane
UV-induced cell damage by lipid peroxidation of the cell membrane. Melanin pigments and their precursors, in particular, pheomelanin and its precursor intermediate, 5-S-cysteinyldopa can become pro-oxidant causing lipid peroxidation in the presence of metal ions, e.g. Fe^{2+}, Fe^{3+} and Cu^{2+} after exposure to UVR.

other research groups have identified lysosome-associated membrane protein (LAMPs) which are associated with the membrane of the two granules[27],[36],[43].

They may derive from the common primordial melanogenesis-associated gene. Repeated exposure of human melanocytes to UVB can directly stimulate the expression of tyrosinase and LAMP gene families. Importantly, tyrosinase and TYRP 1 may coordinate together to up-regulate LAMP 1 molecule which is likely to scavenge some of the toxic species generated during melanin metabolism (hydroxyl radicals) through high content of both N-and O-linked oligosaccharides by continuously coating the inner surface of melanosomal membrane[26],[31],[43].

3．Function and mutation of TYRP genes

Mutations that affect different stages of melanocyte development have been best characterized in experimental mice. The isolation and sequencing of the culprit genes by molecular biology techniques have allowed the determination of the basis of these mutations. The albino mutation of mouse tyrosinase and the brown mutation of Tyrp 1 both alter a cysteine in the EGF motif to serine in albino and different cysteine to tyrosine in brown. Proof of the mutation

status of the alteration in both cases has been provided by analysis of revertants which restore wild type function. In addition, comparison of the phenotypes with those of deletion of the loci indicates that both mutations have complete loss of function of the gene product. On the other hand, DCT (Tyrp 2) containing the slaty mutation, which has arginine to glutamine change at the first copper-biding site may still have considerable DCT activity.

The function of TYRP 1 is still not well characterized. However, it is believed to be involved in eumelanin synthesis since the brown mutation only affects the eumelanic animals. Jackson et al. demonstrated gene changes in Tyrp 1 mRNA expression and in Tyrp 1 gene structure in certain mouse brown b-locus mutants[22]. These findings have provided additional evidence of allelism and allowed an explanation of the phenotypes. The human homologue of TYRP 1 of the mouse brown gene maps to the short arm of chromosome 9 and extends the known region of homology with mouse chromosome 4.

Both recessive and dominant mutations of Tyrp 1 gene have been examined. Some recessive mutations involve single amino acid substitutions, changing an arginine residue to the single sequence cysteine, whereas others affect the

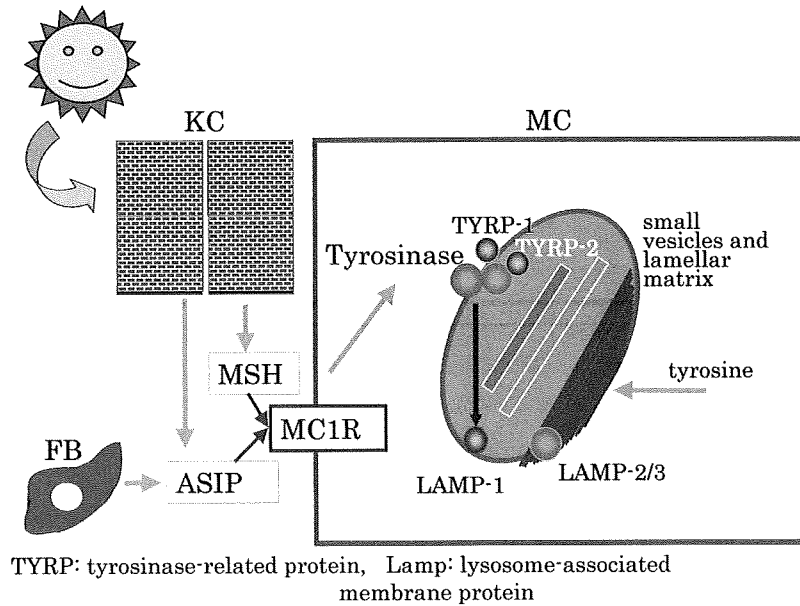TYRP: tyrosinase-related protein, Lamp: lysosome-associated
membrane protein

Figure 6 : Coordinated expression of tyrosinase and LAMP gene family proteins in melanogenesis
cascade
Pheomelanin biogenesis occurs predominantly in red/blond hair follicles. It is not yet clarified
what signals and how the epidermal melanocytes carry out pheomelanin biosynthesis in the skin
of these red/blond haired subjects, though pheomelanin is produced together with eumelanin by
the same melanocyte in the skin. There will be an increased coordinated upregulation in the ex-
pression of TYRP and LAMP gene family proteins after UV exposure.

levels of Tyrp 1 mRNA present in the melano-
cytes. These different mutations result in either
complete loss of function, partial loss of function
or temperature sensitive function. Dominant
mutations affecting the Tyrp 1 gene have also
arisen as a result of a base pair mutation. This
type of mutation may destabilize the melanoso-
mal membrane and allow the intermediates of
melanogenesis, which are normally sequestered
in the melanosomal compartment, to interfere
with normal melanocyte function. Another type
of dominant mutation may arise due to the
Tyrp 1 gene having undergone some re-ar-
rangement, as a result Tyrp 1 is not properly
transcribed, leading to melanocyte dysfunction
and death. It has been therefore suggested that
mutant TYRP 1 protein is involved in toxicity of
melanocytes which is associated with inherently
toxic melanogenesis process[28],[31].

4 . Function and mutation of LAMP genes
    The involvement of lysosomal constituents
including lysosomal enzymes in melanogenesis
has long been implicated. As early as 1968,

Novikoff observed the identical distribution of
tyrosinase (dopa oxidase) and lysosomal acid
phosphatase in the GERL (Golgi-endoplasmic
reticulum-lysosome) areas under electron mi-
croscopy and proposed that melanosomes have
the same developmental sequences as lysosomal
granules do. The compartment of both melano-
somes and lysosomes is acidic. LAMP 1 and
probably LAMP 2 are "household genes" located
in lysosomes, constituting a major portion of ly-
sosome-associated membrane proteins. LAMP 1
and LAMP 2 have similar structures and
masses (up to 90-120 kDa). The deduced amino
acid sequences that a major portion of LAMP 1
and LAMP 2 molecules is exposed continuously
in the lumina of lysosomes, and that this protein
is extensively glycosylated by both N- and O-
glycans. This luminal domain is followed by sin-
gle membrane-spanning domain and a short-cy-
toplasmic tail. This structural organization is
well conserved among molecules of different
species, as well as between LAMP 1 and LAMP 2.
The molecules of LAMP 1 and LAMP 2 have
been suggested, because of their abundance in

lysosomes, to form a nearly continuous coat on the inner surface of the lysosomal membrane which serves as a barrier to soluble lysosomal hydrolases. Heavy glycosylation, including bulky poly-N-acetyl lactosamines (18 N-linked oligosaccharides), probably plays an important role in protecting LAMP molecules from the cytotoxic action of hydrolases (Fig. 6).

Comparison of LAMP 1 and LAMP 2 amino acid sequences revealed that they are encoded by separate genes located on different chromosomes and most likely produced by the duplication of a primordial gene, which took place early in evolution. Thus, LAMP 1 and LAMP 2 could have distinct functions. According to this view, the human LAMP 1 gene is located at chromosome 13 q 34, whereas the human LAMP 2 gene is located at chromosome Xq 24-25. The human LAMP 1 gene is characterized by having a long intron 4, whereas the exons V-IX are present as a cluster. In contrast, the human LAMP 2 gene is characteristic in having a very long intron 8, and exons IV-VIII are present as a cluster. It was shown that LAMP 1 is constitutively synthesized, whereas the synthesis of LAMP 2 is increased during the differentiation of certain embryonic or carcinoma cells. At the present time, we do not know how the mutation of LAMP gene family affects the melanogenesis, although they should have significant influence and have been implicated clinically in abnormal pigmentation seen in such diseases as hypomelanotic macules of vitiligo and café-au-lait macules of Von Recklinghausen's disease[32].

Pheomelanin biosynthesis in EMU and ag-ing of skin

1. Assay of melanin and high content of pheomelanin in melanoma and its precursors

A simple, rapid and sensitive method for the quantitative analysis of eu- and pheomelanin in tissues which makes the isolation of melanin unnecessary[18],[20]. The method is based on the formation of pyrole-2, 3,5-tricarboxylic acid (PTCA) from eumelanin by permanganate oxidation, and aminohydroxyphenylalanine isomers (AHP) from pheomelanin by hydriodic acid hydrolysis. The products are separated and calculated by high-pressure liquid chromatography (HPLC).

The HPLC analysis of melanin has been successfully applied to examine eu- and phe-

nomelanin in the *in vivo* and in vitro cells and tissues[18],[21], human hair[23], mouse hair[8],[19], and cultured melanocytes.[17] The content of dopa and 5-S-cysteinyldopa in both the culture medium and the cells has been used as a marker of differentiation of melanoma cells[2],[3].

Our previous electron microscopic studies[51] showed that melanocytes of dysplastic melanocytic nevi (DMN) were rich in abnormal melanosomes which exhibited features consistent with pheomelanosomes. A significantly high content of pheomelanin was found in DMN lesions, indicating that these abnormal melanosomes may be pheomelanic[16]. UV sensitivity in fair-skinned subjects at high risk for melanoma was found to be associated with high pheomelanin and low eumelanin levels[52]. Epidemiologic data revealing that fair-skinned individuals are more susceptible to skin cancers[1],[11] are linked to greater phototoxicity of pheomelanin (Table II)[53]. In contrast, an examination of eumelanin and pheomelanin concentrations in human skin before and after exposure to UVR showed that factors other than the amount of pheomelanin may be important in determining cancer susceptibility[16]. Ye et al. found that different molecular constituents in pheomelanin are responsible for emission, transient absorption and oxygen photo-consumption, indicating the necessity of combining results from many techniques when trying to develop a unified view of pigment reactivity and electronic structure[55]. It would be important to examine the type of melanogenesis with respect to the degree of skin damage and abnormal pigmentation in the photo-aged skin.

2. UV photoproducts of melanin pigmentation and cytotoxicity

Relatively pure eumelanin and pheomelanin have been isolated and, when subjected to UVR, behave quite differently Menon IA il[48]. investigated the possibility that UVR in the presence of pheomelanin may be more harmful to cells than UVR in the presence of eumelanin. It appears that the production of a short-lived singlet oxygen and its conversion to hydroxyl radicals by the photo-oxidation of pheomelanin are well established[40],[51]. The effects of UVR and visible light upon Ehrlich ascites carcinoma cells in the presence of the melanin isolated from human black hair (eumelanin) or from red hair (pheomelanin) were investigated. UV irradiation of these cells was found to produce cell ly-

sis. The effects were more pronounced when UVR was done in the presence of pheomelanin from red hair than in the presence of black hair eumelanin. Irradiation of the cells in the presence of red hair pheomelanin also decreased the transplantability of these cells. Ehrlich ascites carcinoma cells were injected into mice intraperitoneally after UV irradiation in the presence of eumelanin or pheomelanin. The ability of such treated cells to grow was assessed by changes in animal weight. It was found that carcinoma cells subjected to UVR in the presence of pheomelanin showed impaired growth, which was not seen with UVR alone or UVR in the presence of eumelanin.

Another recent study[44] showed that, when treated with UVA radiation, human red hair melanin was considerably more damaging to Ehrlich ascites cells than eumelanin from black hair. Peritoneal rat mast cells, incubated with pheomelanin and irradiated with UVR, released histamines without cell lysis, whereas such changes did not occur in the presence of eumelanin. These findings may have clearly shown the different biological effect of eumelanin and pheomelanin. It is also important to note that the precursors of these two melanin pigments behave dual role of phototoxic and photoprotective agents[48].

3. UV-photoproducts of pheomelanin in aging process
   Electron-spin resonance spectroscopy ex-

periments by Sealy et al[50]. on black and red melanins, suggested that red melanin (pheomelanin) contained a specific kind of free radical (s) not present in black eumelanin[11], finding that pheomelanin was photo-destroyed, in the presence of oxygen, by UVR. Harsanyi et al.,[16] using the reversion test of Ames, demonstrated that pheomelanin became mutagenic after exposure to UVR[31], describing photo-initiated DNA damage by melanogenic intermediates of 5-S-cysteinyldopa origin. The binding of these molecules to DNA was activated by 300 nm UVR and resulted in single-strand breaks.

Catalase structure and activity was seriously affected by photo-oxidation of its own substrates, hydrogen peroxide, owing to cleavage of its porphyrin active site. Recently the over-expression of mitochondrial catalase in the murine model increased the lifespan of the mice by 40%, indicating the importance of this enzyme in the aging process[49]. Importantly UVA-irradiated pheomelanin altered the structure of catalase and decrease its activity in human skin[37]. It would be interesting to see to what extent UV-photoproducts of pheomelanin are involved in aging process of the skin. It is likely that they will be significantly involved in Caucasians with light-skin and blue eyes, having significant alterations of MC 1 R and pheomelanin in skin and hair, and high risk for developing melanoma (Fig. 7) .
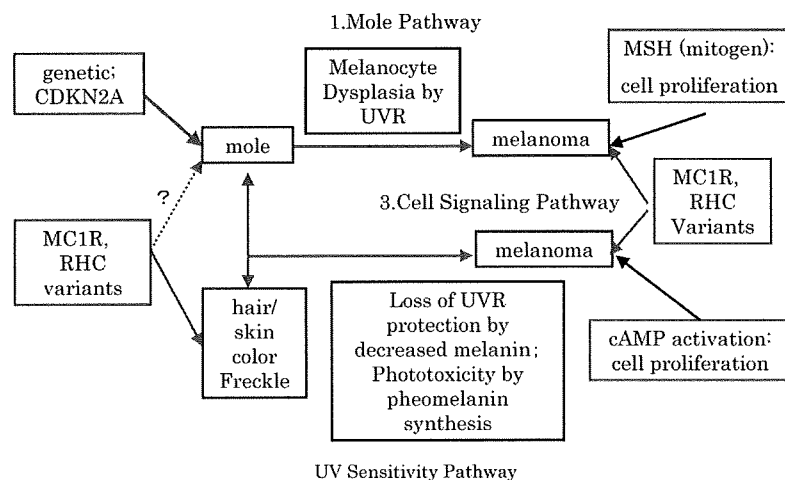

Figure 7 : Involvement of Red hair phenotype and pheomelanin biosynthesis in melanoma development. The figure was modified from Sturn RA (Sturn RA, Melanoma Res 12 : 405-16, 2002).